FDCs express clusterin (current study and reference [12]), and its expression appears to be up-regulated during TSE disease, it is plausible that clusterin is likewise released by FDCs as an activating factor for themselves and/or neighbouring germinal centre B cells [12], which might accelerate abnormal PrP accumulation.

In the Peyer's patches and appendices, some lymphoid follicles showed no detectable PrP deposition, but revealed enhanced clusterin immunoreactivity. Although it is possible that small amounts of undetectable abnormal PrP molecules were present in these follicles, enhanced clusterin expression at this site was probably due to non-specific immune stimulation. Clusterin-enhanced lymphoid follicles were confirmed even in the Peyer's patches of non-infected control mice and in the appendices of non-CJD control cases. The continual exposure of the intestinal lymphoreticular system to a variety of antigens or stress conditions might account for the enhanced clusterin expression in non-TSE affected subjects in comparison with the spleens. The reasons why the regulation of clusterin expression on FDCs in the intestine and other lymphoid tissues appears to differ in uninfected hosts are unknown and therefore worthy of further investigation.

We employed a detergent autoclaving method for PrP detection in this study and found that this method significantly improved sensitivity, especially when analysing the lymphoreticular pathology of TSEs. The early detection of PrP accumulation on FDCs might aid the detection of scrapie transmissibility, and the diagnosis of human variant CJD, for example on tonsil biopsy specimens. Detergent autoclaving also provides a less harsh pretreatment for antigen retrieval, avoids tissue damage, and reduces non-specific background staining. Prolonged formalin fixation of tissue samples results in a considerable reduction of PrP immunoreactivity. This effect might be overcome by modifying the concentration of detergents and/or autoclaving time without causing significant tissue damage.

In conclusion, we have demonstrated that clusterin expression was increased in association with abnormal PrP deposits not only in the CNS [13] but also in the peripheral lymphoreticular system. The observed co-localization and correlative expression of these proteins implies that clusterin might have an important role in PrP pathogenesis in the TSEs, perhaps as a chaperone-like molecule. In keeping with this suggestion, Kempster and associates reported that clusterin-deficient mice inoculated i.p. with mouse-passaged BSE agent had an increased incubation time in comparison with wild-type mice [31]. Thus clusterin might influence the accumulation and/or aggregation of PrP on FDCs, and affect disease progression. Comparative transmission studies using clusterin-deficient mice inoculated with a variety of TSE agent strains by various peripheral routes of exposure will provide further insights into the role of clusterin in TSE pathogenesis.

Acknowledgements

This work was supported by grants to K Doh-ura and T Iwaki from the Ministry of Health, Labour and Welfare, Japan and a grant to K Sasaki from the Japan Society for the Promotion of Science. We thank Ms K Hatanaka, Ms S Nagae, and Mr S Mawatari for their excellent technical assistance. Part of this study was carried out at the Morphology Core, Graduate School of Medical Sciences, Kyushu University. LTβR-Ig and Hu-Ig were kindly provided by Dr Jeffrey Browning (Biogen Inc, Cambridge, MA, USA) and requests for these reagents should be addressed to Jeff_Browning@biogen.com.

References

1. Collinge J, Sidle KC, Meads J, Ironside J, Hill AF. Molecular analysis of prion strain variation and the aetiology of 'new variant' CJD. *Nature* 1996;**383:**685–690.
2. Bruce ME, Will RG, Ironside JW, McConnell I, Drummond D, Suttie A, *et al.* Transmissions to mice indicate that 'new variant' CJD is caused by the BSE agent. *Nature* 1997;**389:**498–501.
3. Hill AF, Desbruslais M, Joiner S, Sidle KC, Gowland I, Collinge J, *et al.* The same prion strain causes vCJD and BSE. *Nature* 1997;**389:**448–450, 526 .
4. Hill AF, Zeidler M, Ironside J, Collinge J. Diagnosis of new variant Creutzfeldt-Jakob disease by tonsil biopsy. *Lancet* 1997;**349:**99–100.
5. Kitamoto T, Muramoto T, Mohri S, Doh-Ura K, Tateishi J. Abnormal isoform of prion protein accumulates in follicular dendritic cells in mice with Creutzfeldt-Jakob disease. *J Virol* 1991;**65:**6292–6295.
6. van Keulen LJ, Schreuder BE, Meloen RH, Mooij-Harkes G, Vromans ME, Langeveld JP. Immunohistochemical detection of prion protein in lymphoid tissues of sheep with natural scrapie. *J Clin Microbiol* 1996;**34:**1228–1231.
7. Jeffrey M, McGovern G, Goodsir CM, Brown KL, Bruce ME. Sites of prion protein accumulation in scrapie-infected mouse spleen revealed by immuno-electron microscopy. *J Pathol* 2000;**191:**323–332.
8. Race R, Oldstone M, Chesebro B. Entry versus blockade of brain infection following oral or intraperitoneal scrapie administration: role of prion protein expression in peripheral nerves and spleen. *J Virol* 2000;**74:**828–833.
9. Glatzel M, Heppner FL, Albers KM, Aguzzi A. Sympathetic innervation of lymphoreticular organs is rate limiting for prion neuroinvasion. *Neuron* 2001;**31:**25–34.
10. Tschopp J, Chonn A, Hertig S, French LE. Clusterin, the human apolipoprotein and complement inhibitor, binds to complement C7, C8-beta, and the b domain of C9. *J Immunol* 1993;**151:**2159–2165.
11. French LE, Wohlwend A, Sappino AP, Tschopp J, Schifferli JA. Human clusterin gene expression is confined to surviving cells during in vitro programmed cell death. *J Clin Invest* 1994;**93:**877–884.
12. Huber C, Thielen C, Seeger H, Schwarz P, Montrasio F, Wilson MR, *et al.* Lymphotoxin-beta receptor-dependent genes in lymph node and follicular dendritic cell transcriptomes. *J Immunol* 2005;**174:**5526–5536.
13. Sasaki K, Doh-ura K, Ironside JW, Iwaki T. Increased clusterin (apolipoprotein J) expression in human and mouse brains infected with transmissible spongiform encephalopathies. *Acta Neuropathol (Berl)* 2002;**103:**199–208.
14. Wilson MR, Easterbrook-Smith SB. Clusterin is a secreted mammalian chaperone. *Trends Biochem Sci* 2000;**25:**95–98.
15. Sasaki K, Doh-ura K, Wakisaka Y, Iwaki T. Clusterin/apolipoprotein J is associated with cortical Lewy bodies: immunohistochemical study in cases with alpha-synucleinopathies. *Acta Neuropathol (Berl)* 2002;**104:**225–230.
16. Chiesa R, Angeretti N, Lucca E, Salmona M, Tagliavini F, Bugiani O, *et al.* Clusterin (SGP-2) induction in rat astroglial

cells exposed to prion protein fragment 106–126. *Eur J Neurosci* 1996;**8:**589–597.
17. McHattie S, Edington N. Clusterin prevents aggregation of neuropeptide 106–126 in vitro. *Biochem Biophys Res Commun* 1999;**259:**336–340.
18. Fischer M, Rulicke T, Raeber A, Sailer A, Moser M, Oesch B, *et al.* Prion protein (PrP) with amino-proximal deletions restoring susceptibility of PrP knockout mice to scrapie. *EMBO J* 1996;**15:**1255–1264.
19. Thackray AM, Klein MA, Bujdoso R. Subclinical prion disease induced by oral inoculation. *J Virol* 2003;**77:**7991–7998.
20. Race RE, Priola SA, Bessen RA, Ernst D, Dockter J, Rall GF, *et al.* Neuron-specific expression of a hamster prion protein minigene in transgenic mice induces susceptibility to hamster scrapie agent. *Neuron* 1995;**15:**1183–1191.
21. Mabbott NA, Mackay F, Minns F, Bruce ME. Temporary inactivation of follicular dendritic cells delays neuroinvasion of scrapie. *Nat Med* 2000;**6:**719–720.
22. Mabbott NA, Young J, McConnell I, Bruce ME. Follicular dendritic cell dedifferentiation by treatment with an inhibitor of the lymphotoxin pathway dramatically reduces scrapie susceptibility. *J Virol* 2003;**77:**6845–6854.
23. Mabbott NA, Williams A, Farquhar CF, Pasparakis M, Kollias G, Bruce ME. Tumor necrosis factor alpha-deficient, but not interleukin-6-deficient, mice resist peripheral infection with scrapie. *J Virol* 2000;**74:**3338–3344.
24. Kitamoto T, Shin RW, Doh-ura K, Tomokane N, Miyazono M, Muramoto T, *et al.* Abnormal isoform of prion proteins accumulates in the synaptic structures of the central nervous system in patients with Creutzfeldt-Jakob disease. *Am J Pathol* 1992;**140:**1285–1294.
25. Bell JE, Gentleman SM, Ironside JW, McCardle L, Lantos PL, Doey L, *et al.* Prion protein immunocytochemistry — UK five centre consensus report. *Neuropathol Appl Neurobiol* 1997;**23:**26–35.
26. Wellmann A, Thieblemont C, Pittaluga S, Sakai A, Jaffe ES, Siebert P, *et al.* Detection of differentially expressed genes in lymphomas using cDNA arrays: identification of clusterin as a new diagnostic marker for anaplastic large-cell lymphomas. *Blood* 2000;**96:**398–404.
27. Whipple EC, Shanahan RS, Ditto AH, Taylor RP, Lindorfer MA. Analyses of the in vivo trafficking of stoichiometric doses of an anti-complement receptor 1/2 monoclonal antibody infused intravenously in mice. *J Immunol* 2004;**173:**2297–2306.
28. Mackay F, Browning JL. Turning off follicular dendritic cells. *Nature* 1998;**395:**26–27.
29. Mabbott NA, Bruce ME. Complement component C5 is not involved in scrapie pathogenesis. *Immunobiology* 2004;**209:**545–549.
30. Zlokovic BV. Cerebrovascular transport of Alzheimer's amyloid beta and apolipoproteins J and E: possible anti-amyloidogenic role of the blood-brain barrier. *Life Sci* 1996;**59:**1483–1497.
31. Kempster S, Collins ME, Aronow BJ, Simmons M, Green RB, Edington N. Clusterin shortens the incubation and alters the histopathology of bovine spongiform encephalopathy in mice. *Neuroreport* 2004;**15:**1735–1738.

Neuropathology 2006; **26**, 82–88 doi:10.1111/j.1440-1789.2006.00638.x

Case Report

Increased asymmetric pulvinar magnetic resonance imaging signals in Creutzfeldt–Jakob disease with florid plaques following a cadaveric dura mater graft

Yoshinobu Wakisaka,[1,2] Naohiko Santa,[2,3] Katsumi Doh-ura,[4] Tetsuyuki Kitamoto,[4] Setsuro Ibayashi,[2] Mitsuo Iida[2] and Toru Iwaki[1]

[1]Department of Neuropathology, Neurological Institute, and [2]Department of Medicine and Clinical Science, Graduate School of Medical Sciences, Kyushu University, Fukuoka, [3]Cerebrovascular Department, Neuroscience Institute, St Mary Hospital, Kurume, and [4]Department of Prion Research, Tohoku University Graduate School of Medicine, Sendai, Japan

A 9-year-old Japanese girl received a cadaveric dura mater graft during surgery following a head injury with brain contusion. She continued to do well, but when she became 19-years-old, she gradually showed a violent character and was treated in a psychiatric hospital. Another 6 years later, 200 months after the procedure, she developed a progressive gait ataxia, which subsequently led to her death within 10 months of onset. An autopsy showed she had CJD. This patient represents an atypical case of dura-associated CJD (dCJD) with unusual clinicopathological features including the late occurrence of myoclonus, an absence of periodic synchronous discharges in the electroencephalogram, and the presence of widespread florid plaques. However, our detection of an asymmetrical increase in the MRI-derived images of pulvinar nuclei has not been previously observed in other atypical cases of dCJD. Because atypical dCJD cases share several clinicopathological features with those of vCJD, and because asymmetrical hyperintense signals in the pulvinar have been observed in some neuropathologically confirmed vCJD cases, we had some difficulty in a differential diagnosis between atypical dCJD and vCJD. This is the first atypical dCJD case showing a pulvinar high signal compared with all other basal ganglia on MRI.

Key words: CJD, dura graft, MRI, pulvinar sign, vCJD.

Correspondence: Dr Yoshinobu Wakisaka, MD, PhD, Department of Medicine and Clinical Science, Graduate School of Medical Sciences, Kyushu University, 3-1-1 Maidashi, Higashi-ku, Fukuoka, 812-8582, Japan. Email: w-yoshi@intmed2.med.kyushu-u.ac.jp

Received 21 January 2005; revised and accepted 11 April 2005.

INTRODUCTION

Most dura-associated CJD (dCJD) cases have similar clinicopathological features to sporadic CJD (sCJD), presenting progressive mental deterioration, ataxia, myoclonus and characteristic EEG findings such as periodic discharges.[1] However, some patients with atypical dCJD exhibit clinicopathological features distinct from those of most dCJD cases have some resemblance to vCJD cases; that is, a slow progressive clinical course with the absence or late occurrence of periodic discharges on EEG, and the presence of widespread florid plaques in addition to widespread spongiform change, neuronal loss and astrocytosis.[2–8] On the other hand, the radiological features are different between atypical dCJD and vCJD cases. While vCJD cases present pulvinar high signals compared to all other basal ganglia,[9,10] atypical dCJD cases have not been reported to show such hyperintensity in pulvinar nuclei.[2–8] Moreover, the pathological features of the pulvinar nuclei are also different between atypical dCJD and vCJD cases. Here, we report an atypical dCJD case presenting asymmetrical pulvinar hyperintensity on MRI with different pathological characteristics of the pulvinar nucleus from those of reported atypical dCJD and vCJD cases.

CLINICAL SUMMARY

In November 1985, a 9-year-old Japanese girl received a cadaveric dural graft (Lyodura, B Braun Melsungen AG, Germany) at left frontotemporal region following a head injury with brain contusion. Six months later, she had a seizure and anti-epileptic drugs were administered. However, she did not take anti-epileptic drugs regularly, and epilepsy

frequently occurred. From 1995, she gradually developed a violent character. She was diagnosed as suffering a post-traumatic psychosis and received treatment in a psychiatric hospital. In June 2002, 200 months after the procedure, she began to develop an ataxic gait and became bed-ridden. By January 2003, she gradually showed memory disturbance and lost her spontaneous speech and was unable to communicate. She also exhibited myoclonic jerks in her upper limbs. She frequently suffered from aspiration pneumonia, and was brought to our hospital for respiratory insufficiency on 9 April 2003. On admission, she was akinetic and mute with decorticate posturing. There was no apparent history of depression, anxiety, apathy or delusions. Neurological examination showed moderate rigidity in bilateral upper and lower extremities, and myoclonus in bilateral upper extremities. The light reflex, corneal reflex and oculocephalic reflex were all normal. The motor and sensory systems could not be examined in detail. Deep tendon reflexes were normal. There was slow activity without any periodic discharge in her EEG. One week before her death, T2-weighted and proton density-weighted brain MRI showed significant hyperintensity in the thalamic pulvinar nuclei, which was predominantly on the left side, and moderate hyperintensity of the basal ganglia (Fig. 1A,B). Diffusion-weighted and gadolinium(III)-diethyltriaminepentaacetic acid (Gd-DTPA)-enhanced MRI revealed hyperintense signals in the pulvinar (Fig. 1C,D). The brain MRI also presented hyperintense signal by T2-weighted and proton density-weighted images and hypointense signal by diffusion-weighted and Gd-DTPA-enhanced images at the left frontal lobe, corresponding to where the brain contusion existed. In addition, Gd-DTPA enhanced images revealed hyperintense signals at the margin of the brain contusion. Based on the findings of the brain MRI, the diagnosis of dCJD was suspected. However, her respiratory insufficiency progressively worsened and she developed septic shock. Therefore, we could not assess further examination including the cerebrospinal fluid level of the 14-3-3 protein. She died on 19 April, 2003, 10 months after the onset of ataxic gait. The patient's family gave informed consent for the genetic and postmortem studies.

PATHOLOGICAL FINDINGS, IMMUNOBLOTTING AND GENE ANALYSIS

On examination, her brain weighed 1120 g, and there was a large defect in the left basal forebrain. While cerebral atrophy was not obvious, there was substantial atrophy of the cerebellum. The right side of the half-brain was deep-frozen for biochemical examination, and the other half was fixed in buffered formalin. Microscopically, most cerebral cortices had mild to moderate spongiform changes, neuronal loss, and astrocytosis with a predilection for the deep cortical layers. In contrast, the cingulate gyrus and insular cortex exhibited moderate to severe pathological changes throughout the whole layers. The putamen showed moderate spongiform change, neuronal loss and astrocytosis. Anterior nucleus of the thalamus presented mild spongiform change and neuronal loss, and moderate astrocytosis. Ventral lateral nucleus and dorsomedial nucleus of the thalamus displayed mild spongiform change, moderate neuronal loss and astrocytosis. Pulvinar nucleus of the thalamus exhibited the most severe neuronal loss and spongiform change, and greater astrocytosis than the cerebral cortices (Table 1). The hippocampus was almost completely spared. In the cerebellum, moderate atrophy of the molecular layer was associated with mild spongiform change and astrocytosis, while moderate neuronal loss of the granule layer and severe neuronal loss of the dentate nucleus was associated with moderate astrocytosis. The Purkinje cells were almost completely preserved. In HE sections, we frequently noted Kuru plaques in a number of regions of the cerebral cortex, the putamen and the pulvinar nucleus of the thalamus. The cores of the plaques were stained with PAS, and, when stained with Congo red, appeared apple green in polarized light. In addition, many of the Kuru plaques were surrounded by a zone of vacuolar change, consistent with florid plaques, which are known hallmarks of vCJD. Although the pulvinar nucleus of the thalamus presented frequent Kuru plaques, there were only a few plaques in anterior, ventral lateral and dorsomedial nuclei of the thalamus. Immunohistochemistry for PrP revealed widespread synaptic staining and numerous plaque-like deposits, including florid plaques in all areas of the cerebral cortices, putamen, pulvinar nucleus of the thalamus and white matter of the cerebellum. The globus pallidus, the anterior, ventral lateral and dorsomedial nuclei of the thalamus, and molecular layer of the cerebellum mainly showed synaptic staining associated with mild granular prion protein depositions. In addition, there were PrP deposits surrounding blood vessels, neuronal cell bodies and processes in the cerebral cortex and in the pulvinar nucleus (Fig. 2). The region around the head injury with brain contusion showed mild spongiform change with severe astrocytosis. Only a few Kuru plaques were found in this region (Table 1).

The sequence analysis of prion protein gene (*PRNP*) derived from the brain tissue showed no mutation with homozygous for methionine at codon 129 or for glutamate at codon 219, which are polymorphic sites of the *PrP* gene. Immunoblotting for the abnormal prion protein in the brain demonstrated a type 1 prion protein glycoform pattern (Parchi's classification)[11] (Fig. 3). The final diagnosis was atypical dCJD.

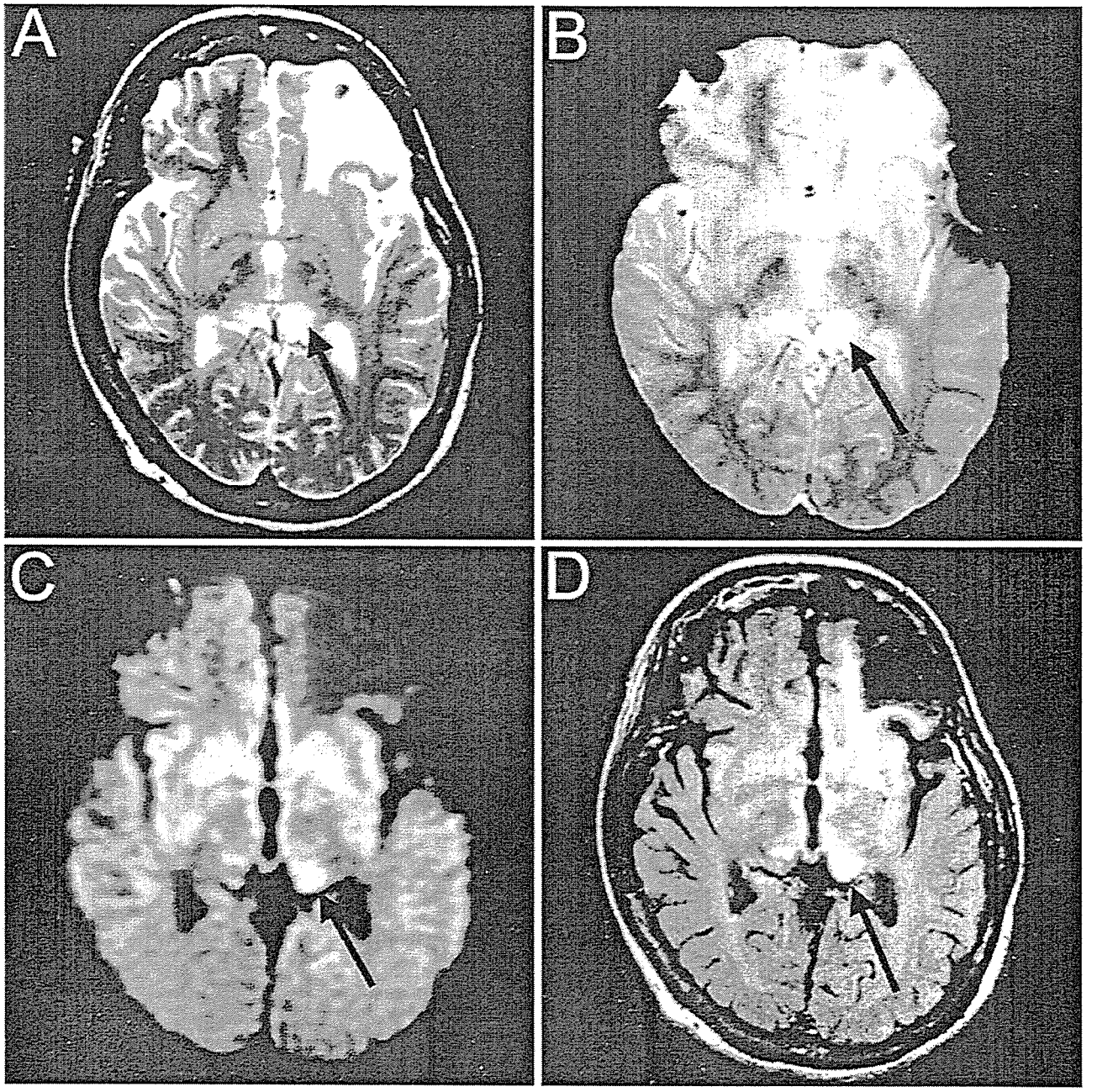

Fig. 1 Neuroradiological images. (A) T2-weighted image, (B) proton density-weighted image, (C) diffusion-weighted image, and (D) gadolinium(III)-diethyltriaminepentaacetic acid (Gd-DTPA)-enhanced brain MRI obtained 1 week prior to death. The images reveal hyperintensity in the pulvinar of the thalamus, and is more apparent in the left side (arrows). Images also show intense bilateral signals in the caudate nuclei and putamen.

DISCUSSION

We present the first atypical dCJD case to show a high pulvinar signal compared with all other basal ganglia on MRI, prominent lesions with severe spongiform changes, neuronal loss and numerous florid plaques in the posterior thalamus at autopsy.

Most dCJD cases take the form of typical sCJD.[1] Most dCJD cases are clinically evident as a progressive mental deterioration, ataxia and myoclonus. Periodic discharges

are often noted in the EEG before the terminal stage of the clinical course. The disease often progresses rapidly and the clinical course lasts less than 2 years. MRI of dCJD cases has previously shown either normal or non-specific and diffuse brain atrophy.[12] T2-weighted MRI has also shown sCJD cases frequently exhibit symmetrical and hyperintense changes in the putamen and caudate head compared with the thalamus and cerebral cortex.[13,14] In cases of sCJD, high-intensity signals in the cerebral and cerebellar cortex are also occasionally seen in fluid-attenuated inversion recovery, proton density-weighted and diffusion-weighted MRI-derived images.[13] Pathologically, the cerebral cortex and cerebellum of dCJD cases are substantially affected. Severe spongiform changes, astrocytosis and neuronal loss are found throughout the brain and cause substantial atrophy, resulting in brain weights of less than 1000 g. Immunohistochemistry reveals diffuse synaptic type deposition of PrP. None or few amyloid plaques are found in the brain.

However, among more than 110 alleged dCJD cases,[15] there have been some atypical dCJD patients with clinicopathological features which are different from those of sCJD and most dCJD cases but share several features with those of vCJD.[2–8] These atypical dCJD and vCJD cases show a slowly progressive clinical course reaching the state of akinetic mutism. The reported duration of atypical dCJD were ranged 5–24 months.[2–8] This duration resembled cases of vCJD, whose duration ranged 8–38 months.[16] In addition, periodic discharges on EEG were commonly absent in both atypical dCJD and vCJD cases. On the other hand, there are several different clinical features between these cases. While most atypical dCJD cases present initially with ataxia and mental deterioration, such as disorientation or memory disturbance often following the ataxia,[2–8] many vCJD cases initially suffer from sensory symptoms including persistent limb pain and/or persistent psychiatric symptoms as depression, anxiety, apathy and withdrawal.[16] Ataxia was reported to develop about 6 months after the onset of psychiatric and sensory symptoms.[16] Moreover, although myoclonus is absent or occurred at the end stage of the disease in atypical dCJD cases, involuntary movements including myoclonus are commonly noted during the clinical course of vCJD cases.[16] The duration of the disease of our case and the absence of periodic discharges on EEG were similar to those features of atypical dCJD and vCJD cases. On the other hand, because our case presented progressive cognitive impairment after the onset of ataxia, and because myoclonus was absent until the end stage of the disease, the clinical course of our case more resembled those of atypical dCJD than vCJD cases.

Pathologically, most atypical dCJD and vCJD cases show widespread spongiform change, neuronal loss and astrocytosis. These pathological changes are mild in the cerebral cortex and severe in caudate nucleus, putamen and cerebellum in both atypical dCJD and vCJD cases.[2–8]

Table 1 Neuropathological findings of left side of the half brain

	Spongiform change	Neuronal loss	Astrocytosis	Kuru plaques
MFG	+++	+	++	+++
MTG	+	+	++	++
IPG	+	+	++	+
PVC	+	+	+	++
Cingulate gyrus	+++	++	++	++
Insular cortex	++	++	++	+++
Hippocampus	–	–	–	–
Globus pallidus	+	+	+	–
Putamen	++	++	++	++
Thalamus AN	+	+	++	+
DMN	+	++	++	+
VLN	+	++	++	+
PN	+++	+++	+++	+++
Contusion area	+		+++	+
Cerebellum ML	+		+	–
PCL		–		
GL		++	++	
WM			++	+
DN		+++	++	–

MFG, middle frontal gyrus; MTG, middle temporal gyrus; IPG, Inferior parietal gyrus; PVC, primary visual cortex of occipital lobe; AN, anterior nucleus; DMN, dorsomedial neucleus; VLN, ventral lateral nucleus; PN, pulvinar nucleus; ML, molecular layer; PCL, purkinje cell layer; GL, granular layer; WM, white matter; DN, dentate nucleus.

Spongiform change and neuronal loss are absent (–), mild (+), moderate (++), severe (+++) on HE sections. Astrocytosis and Kuru plaques are absent (–), mild (+), moderate (++), severe (+++) on sections of immunohistochemistry probed with an anti-GFAP antibody (polyclonal, DAKO, Glostrup, Denmark) and antiprion protein antibody (monoclonal, clone 3F4, Senetek, Maryland Heights, MO, USA), respectively.

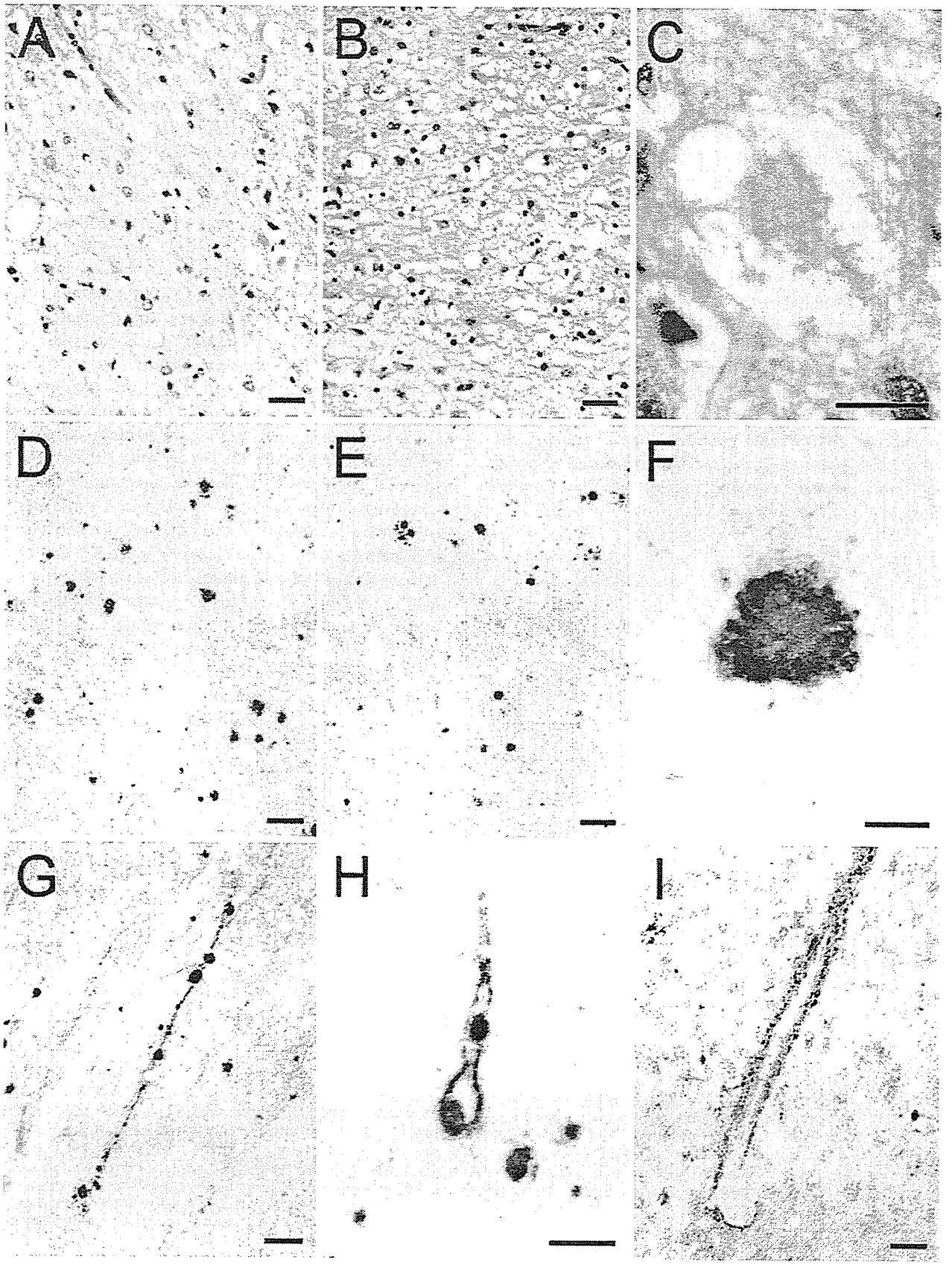

The florid plaques, which are the pathological hallmark of vCJD, are also found in atypical dCJD cases, although they are more abundant in number in vCJD than atypical dCJD cases. These florid plaques distribute widely in the cerebrum and cerebellum but are only occasionally seen in the thalamus in both CJD cases. However, the pathological features of the thalamus are different between these CJD cases. In atypical dCJD cases, spongiform change, neuronal loss and astrocytosis were reported to be intense especially in anterior and medial nuclei.[5] In vCJD cases, while spongiform change is focally seen in anterior and medial thalamic nuclei and pulvinar nuclei are relatively spared from spongiform change, there is extensive neuronal loss with marked astrocytosis in the pulvinar nuclei.[17] In our case, the neuronal loss and astrocytosis were markedly noted in pulvinar nucleus rather than anterior and medial nuclei. Thus, because the pulvinar nucleus of our case presented marked neuronal loss and astrocytosis as well as severe spongiform change and numerous florid plaques, the pathological features of our case was considered to be distinct from those of reported atypical dCJD and vCJD cases.

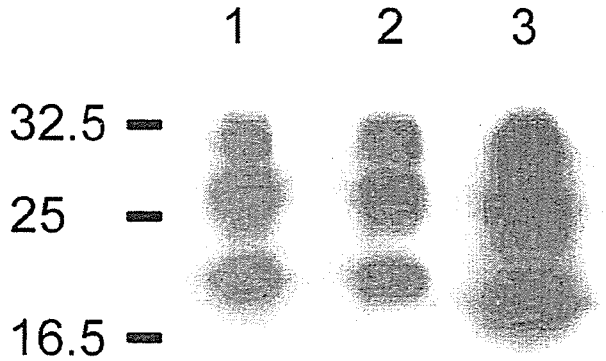

Fig. 3 Immunoblotting. Lane 1, positive control showing type 1 PrP glycoform pattern; lane 2, present study; lane 3, positive control showing type 2 PrP glycoform pattern. The abnormal PrP molecules in the brain homogenates of this case (lane 2) exhibit a type 1 PrP glycoform pattern. Molecular sizes (kDa) are indicated on the left.

Pulvinar increased signals greater than all other basal ganglia on T2-weighted, proton density-weighted, and diffusion-weighted MRI found in our case were unique features and have not been observed in other atypical dCJD cases. The hyperintensity of these images is thought to correlate with the astrocytosis and neuronal loss observed in histological examination.[9] On the other hand, the Gd-DTPA enhancement of the pulvinar nuclei has not been reported in any type of CJD cases. Because the left frontal lesion of the contusion as well as the pulvinar nuclei were enhanced with Gd-DTPA, and because the increased pulvinar signals were asymmetrical and more intense on the left side, these hyperintense signals might reflect damage of the pulvinar nuclei due to a contusion in the left basal forebrain. However, although the thalamus has direct reciprocal connection to the cerebral cortices, the pulvinar nucleus make connections not with the frontal lobe but with the occipital cortex including the striate cortex.[18] In addition, the common pathological findings of the Gd-DTPA-enhancing lesions, the left pulvinar nucleus and the rim of the contusion in the left basal forebrain, was severe astrogliosis. While Gd-DTPA enhancement indicates vascular leakage in general, Gd-DTPA enhancement associated with astrogliosis has also been reported.[19] Therefore, although the precise reason was not clear, we considered that the increased pulvinar signals of our case would reflect pathological changes including severe astrogliosis caused not by traumatic brain injury but by CJD.

The marked pulvinar hyperintensity compared with all other basal ganglia recognized in our case raised the concern of vCJD because the asymmetrical pulvinar hyperintensity has previously been detected in some neuropathologically confirmed vCJD cases.[20] However, the radiological hallmark of vCJD, the pulvinar sign, is defined as symmetrical hyperintensity. Thus, the lack of symmetry in our case was not identical to the radiological features of vCJD cases. In addition, the proposed diagnostic criteria excluded the classification of our case as vCJD after possible iatrogenic exposure.[16] Moreover, the PrP glycoform pattern of our case was type 1 according to Parchi's classification, and was identical to those of reported atypical dCJD cases but was completely different from that of vCJD.[1]

Fig. 2 Verification of abnormal PrP deposition by histological examination. (A–C) HE staining. (D–I) Immunohistochemistry probed with an anti-prion protein antibody (monoclonal, clone 3F4, Senetek, Maryland Heights, MO, USA). Severe spongiform change, neuronal loss, and astrocytosis occurred in the left middle frontal lobe (A) and left pulvinar nucleus of the thalamus (B). (C) A prion protein plaque is surrounded by spongiform changes, to give the appearance of a florid plaque in the pulvinar nucleus. There are many prion plaques in the left middle frontal lobe (D) and in the left pulvinar nucleus of the thalamus (E). (F) The core of the florid plaque is intensely immunostained. (G) Unique prion protein depositions are linearly aligned with the neuronal axon in the left cingulate gyrus. (H) Prion protein deposition occurred around the neuronal cell body and process in the left cingulate gyrus. (I) Granular prion protein deposits are present around the wall of a blood vessel in the left pulvinar nucleus of the thalamus. Bars (A,B,D,E,H) 30 μm, (C,F) 15 μm, (G,I) 60 μm.

Therefore, we concluded our case to be atypical dCJD with radiological and pathological characteristics distinct from those of any dCJD cases.

ACKNOWLEDGMENTS

We thank Ms. K. Hatanaka for her excellent technical assitance.

REFERENCES

1. Satoh K, Muramoto T, Tanaka T *et al.* Association of an 11–12 kDa protease-resistant prion protein fragment with subtypes of dura graft-associated Creutzfeldt-Jakob disease and other prion diseases. *J Gen Virol* 2003; **84**: 2885–2893.
2. Kimura K, Nonaka A, Tashiro H *et al.* Atypical form of dural graft associated Creutzfeldt-Jakob disease: report of a postmortem case with review of the literature. *J Neurol Neurosurg Psychiatry* 2001; **70**: 696–699.
3. Kopp N, Streichenberger N, Deslys JP, Laplanche JL, Chazot G. Creutzfeldt-Jakob disease in a 52-year-old woman with florid plaques. *Lancet* 1996; **348**: 1239–1240.
4. Kretzschmar HA, Sethi S, Földvári Z *et al.* Iatrogenic Creutzfeldt-Jakob disease with florid plaques. *Brain Pathol* 2003; **13**: 245–249.
5. Shimizu S, Hoshi K, Muramoto T *et al.* Creutzfeldt-Jakob disease with florid-type plaques after cadaveric dura mater grafting. *Arch Neurol* 1999; **56**: 357–362.
6. Takashima S, Tateishi J, Taguchi Y, Inoue H. Creutzfeldt-Jakob disease with florid plaques after cadaveric dural graft in a Japanese woman. *Lancet* 1997; **350**: 865–866.
7. Lane KL, Brown P, Howell DN *et al.* Creutzfeldt-Jakob disease in a pregnant woman with an implanted dura mater graft. *Neurosurgery* 1994; **34**: 737–740.
8. Mochizuki Y, Mizutani T, Tahiri N *et al.* Creutzfeldt-Jakob disease with florid plaques after cadaveric dura mater graft. *Neuropathology* 2003; **23**: 136–140.
9. Collie DA, Sellar RJ, Zeidler M, Colchester ACF, Knight R, Will RG. MRI of Creutzfeldt-Jakob disease: imaging features and recommended MRI protocol. *Clin Radiol* 2001; **56**: 726–739.
10. Zeidler M, Sellar RJ, Collie DA *et al.* The pulvinar sign on magnetic resonance imaging in variant Creutzfeldt-Jakob disease. *Lancet* 2000; **355**: 1412–1418.
11. Parchi P, Giese A, Capellari S *et al.* Classification of sporadic Creutzfeldt-Jakob disease based on molecular and phenotypic analysis of 300 subjects. *Ann Neurol* 1999; **46**: 224–233.
12. Santos JMG, Corbalán JAL, Martinez-Lage JF, Guillén JS. CT and MRI in iatrogenic and sporadic Creutzfeldt-Jakob disease: as far as imaging perceives. *Neuroradiology* 1996; **38**: 226–231.
13. Schröter A, Zerr I, Henkel K, Tschampa HJ, Finkenstaedt M, Poser S. Magnetic rosonance imaging in the clinical diagnosis of Creutzfeldt-Jakob disease. *Arch Neurol* 2000; **57**: 1751–1757.
14. Yoon SS, Chan S, Chin S, Lee K, Goodman RR. MRI of Creutzfeldt-Jakob disease: asymmetric high signal intensity of the basal ganglia. *Neurology* 1995; **45**: 1932–1933.
15. Brown P, Preece M, Sato T *et al.* Iatrogenic Creutzfeldt-Jakob disease at the millennium. *Neurology* 2000; **55**: 1075–1081.
16. Will RG, Zeidler M, Stewart GE *et al.* Diagnosis of new variant Creutzfeldt-Jakob disease. *Ann Neurol* 2000; **47**: 575–582.
17. Ironside JW, McCardle L, Horsburgh A *et al.* Pathological diagnosis of variant Creutzfeldt-Jakob disease. *APMIS* 2002; **110**: 79–87.
18. Carpenter MB, Sutin J. Diencephalon. In: Carpenter MB, Sutin J (eds). *Human Neuroanatomy*, 8th edn. Baltimore: Williams & Wilkins, 1983; 500–524.
19. Nishimura R, Takahashi M, Morishita S *et al.* MR Gd-DTPA enhancement of radiation brain injury. *Radiat Med* 1992; **10**: 109–116.
20. Collie DA, Summers DM, Sellar RJ *et al.* Diagnosing variant Creutzfeldt-Jakob disease with the pulvinar sign: MR imaging findings in 86 neuropathologically confirmed cases. *Am J Neuroradiol* 2003; **24**: 1560–1569.

Neuropathology 2006; **26**, 43–49 doi:10.1111/j.1440-1789.2006.00654.x

Original Article

Brain stem lesions in sporadic Creutzfeldt–Jakob disease: A histopathological and immunohistochemical study

Masayuki Shintaku,[1] Chikao Yutani[2] and Katsumi Doh-ura[3]

[1]Department of Pathology, Osaka Red Cross Hospital, Tennoji, Osaka, [2]Department of Life Science, Faculty of Science, Okayama University of Science, Okayama, and [3]Department of Prion Research, Tohoku University Graduate School of Medicine, Aoba, Sendai, Japan

Lesions of the brain stem in sporadic CJD were histopathologically and immunohistochemically investigated using an anti-PrP antibody on ten consecutive autopsy cases. Three major histopathological changes, spongiform changes, neuronal loss and hypertrophic astrocytosis, were employed as parameters of the alterations. The quadrigeminal plate and pontine nuclei were the most severely and consistently affected structures, and immunoreactivity against PrP was seen in these structures. There existed some discrepancies between the severity of the lesions and the intensity of the immunoreactivity against PrP. The medulla oblongata essentially remained normal on histopathological examination, but the inferior olivary nucleus showed prominent PrP deposition. Although the general view that pathological alterations in the brain stem are relatively mild in sporadic CJD was confirmed in this study, lesions of variable degrees which might influence a patient's clinical course were still observed in many structures in the brain stem.

Key words: brain stem, CJD, histopathology, immunohistochemistry, PrP.

INTRODUCTION

The principal neuropathological features seen in a brain affected by sporadic CJD include spongiform changes of the neuropil, loss of neurons, proliferation of hypertrophic astrocytes and, in a subset of cases, the formation of amyloid plaque.[1,2] These changes are most prominent in the neocortex of the cerebrum and are also found in various degrees in the basal ganglia and thalamus. In many cases, the cerebellar cortex is also severely affected and, especially in the panencephalopathic type, the white matter of the cerebrum exhibits remarkable pathological alterations.[3] On the other hand, it is believed that pathological alterations in the brain stem below the level of the mesencephalon are mild in sporadic CJD, although involvement of the pontine base or inferior olivary nucleus has been occasionally described.[1,3–5] This is in contrast to other human prion diseases, such as kuru,[6,7] and also prion diseases of animals, such as scrapie,[8] and bovine spongiform encephalopathy (BSE),[9] in which the brain stem is consistently and severely affected by similar pathological processes.

There exist few reports which detail brain stem lesions in sporadic CJD.[10] We investigated such lesions by histopathological and immunohistochemical methods using an anti-PrP antibody on consecutive autopsy cases of sporadic CJD.

MATERIALS AND METHODS

From the autopsy files of the departments of pathology of the Osaka Red Cross Hospital and the National Cardiovascular Center, ten consecutive autopsy cases of sporadic (non-familial and non-iatrogenic) CJD were retrieved. No case of the variant CJD[11,12] was investigated. A summary of the clinicopathological findings of these cases is presented in Table 1. Analysis of the *PrP* gene had been only performed for the recently autopsied cases (cases 8–10), and in all of these the gene was the wild type and codon 129 was homozygous for methionine.

In all cases, the brain had been routinely examined after formalin fixation. Representative sections taken from many regions of the cerebrum and cerebellum were

Correspondence: Masayuki Shintaku, MD, Department of Pathology, Osaka Red Cross Hospital, Tennoji, Osaka 543-8555, Japan. Email: masa-s@sings.jp

Received 28 March 2005; revised and accepted 30 June 2005.

Table 1 Clinicopathological findings of the cases studied

Case	Age (years)	Gender	Duration (months)	Brain weight (grams)	Prion typing
1	70	F	20	830	
2	77	F	7	1110	
3	59	M	24	850	
4	75	F	35	900	
5	66	M	45	860	
6	67	M	18	1010	
7	71	M	16	Unknown	
8	71	M	7	1140	MM1
9	61	F	7	900	MM1
10	56	F	16	790	MM1

reviewed, and the neuropathological diagnosis of sporadic CJD was confirmed. Each brain stem had been cut in planes vertical to the long axis in all cases, and tissue sections had been taken from four to six different levels extending from the rostral mesencephalon to the caudal medulla oblongata. Paraffin sections had then been stained with HE, luxol fast blue-periodic acid-Schiff, modified Bielschowsky, and Nissl stains. We evaluated the lesions of the gray matter of the brain stem employing the following three histopathological parameters:[1,2] (i) spongiform changes of the neuropil; (ii) loss of neurons; and (iii) the proliferation of hypertrophic astrocytes. Other specific pathological alterations were also recorded. Because there was a subtle difference in the examined levels of sections between the cases because of the retrospective nature of this study, only easily identifiable, distinct nuclear groups were selected for evaluation. Changes in the white matter of the brain stem were excluded, because they were considered to largely represent secondary alterations caused by lesions in the cerebral or cerebellar cortex.

In eight cases for which preserved paraffin blocks were available, sections were recut and immunohistochemical investigations were performed using a monoclonal antibody against PrP (clone 3F4, DakoCytomation, Glostrup, Denmark; 1:100) and by employing the Envision Plus detection system (DakoCytomation) after pretreatment of the sections by hydrolytic autoclaving in 1.5 mmol hydrochloric acid at 121°C for 10 min.[13] Paraffin sections of the medulla oblongata were available only for cases 7–10.

The severity of individual lesions and the intensity of the immunohistochemical reactions were evaluated using the four-tiers grading system: (−) absent or negative; (±) equivocal or very weakly positive; (+) definitely present or positive; and (++) severe or intensely positive.

RESULTS

For the overall neuropathological features of the cerebral hemispheres and the cerebellum, in all cases the brain showed gross atrophy, and the thinning of the cerebral cortex was marked. The cerebellum also exhibited severe cortical atrophy along with the marked depopulation of granule cells and thinning of the molecular layer. No amyloid plaque was observed in any case. The white matter of the cerebral hemispheres showed diffuse myelin pallor and axonal loss. In addition, peculiar, localized spongiform changes of the subcortical white matter, which is a characteristic of panencephalopathic type CJD,[3] were noted in cases 9 and 10.

On gross examination, the mesencephalon and pons showed diffuse atrophy of mild to moderate degree in every case, and the pontine base had lost its bulge on the ventral surface. On the other hand, the medulla oblongata appeared almost normal on macroscopic observation. A summary of the brain stem lesions is presented in Table 2.

Mesencephalon

The superior and inferior colliculi were the most distinctly and consistently affected sites among the structures present in the mesencephalon. Spongiform changes were seen chiefly in the superficial layers, and neuronal loss and astrocytosis were found diffusely throughout these structures (Fig. 1). The periaqueductal gray matter was also involved, but less distinctly than in the quadrigeminal plate, and neuronal loss was not apparent. In case 1, a few senile plaques were observed in this region. Neurons of the oculomotor nucleus were well preserved, but spongiform changes were noted in cases 9 and 10. Of special interest, multiple large vacuoles were occasionally found in the neuronal perikarya in the oculomotor nucleus of these two cases (Fig. 2). In another case (case 3), similar vacuoles in the perikarya were found in several pigmented neurons of the substantia nigra. Pathological alterations in the red nucleus and reticular formation were mild except for case 9, in which spongiform changes and astrocytosis were noted to a moderate degree. In the substantia nigra, neuronal loss to a mild degree was noted in the zona compacta in most cases. Spongiform changes were clearly observed in four cases, and a few "foamy spheroids" were

Table 2 Summary of the histopathological and immunohistochemical findings of the brain stem

		Case 1				Case 2				Case 3				Case 4				Case 5			
		SC	NL	AS	PrP	SC	NL	AS	SC	NL	AS	PrP	SC	NL	AS	PrP	SC	NL	AS	PrP
Mesencephalon	Superior colliculus	−	+	++	+	NE	NE	NE	−	±	++	−	NE	NE	NE	NE	+	±	+	+
	Inferior colliculus	NE	NE	NE	NE	+	±	+	NE	NE	NE	NE	NE	NE	NE	NE	NE	NE	NE	NE
	Periaqued. gray matter	−	−	+	±	+	−	−	−	−	+	−	NE	NE	NE	NE	±	−	±	+
	Oculomotor nucleus	−	−	+	−	±	−	−	−	−	−	−	NE	NE	NE	NE	±	−	±	±
	Red nucleus	−	−	+	−	NE	NE	NE	−	−	+	−	±	−	+	−	−	−	±	−
	Reticular formation			+	+	±		±			+		NE	NE	NE	NE			±	±
	Subst. nigra. Z. comp.	−	+	+	−	−	−	−	+	+	+	−	++	+	+	−	++	±	±	±
	Subst. nigra. Z. reticu.	−	+	+	−	−	−	−	+	+	+	−	NE	NE	NE	NE	++	±	±	−
Pons	Locus ceruleus		±	+	+	NE	NE	NE	NE	NE	NE	NE	±	±	±					+
	Raphe nucleus	−	−	−	+	NE	NE	NE	−	−	+	+	±	±	±	−	−	−	−	+
	Reticular formation	−	−	−	+	NE	NE	NE	−	−	−	+	−	−	+	−	−	−	−	+
	Pontine nuclei	−	++	++	+	−	−	−	−	+	++	+	−	++	++	−	++	++	++	±
Medulla oblongata	Nucl. N. hypogloss.	−	±	+	NE	−	−	−	−	−	±	NE	−	−	+	NE	−	−	±	NE
	Nucl. dors. n. trigem.	−	−	−	NE	NE	NE	NE	−	−	±	NE	−	−	+	NE	−	−	±	NE
	Nucl. tr. spin. n. trigem.	−	−	−	NE	−	−	−	−	−	±	NE	−	−	+	NE	−	−	±	NE
	Raphe nucleus	−	−	−	NE	NE	NE	NE	−	−	±	NE	−	−	−	NE	−	−	±	NE
	Reticular formation	−	−	±	NE	−	−	−	−	−	±	NE	−	−	+	NE	−	−	±	NE
	Olivary nucleus			+	NE						+	NE		+	+	NE		+	+	NE
	Nucl. fasc. poster.	−	−	±	NE	−	−	−	−	−	−	NE	−	−	+	NE	NE	NE	NE	NE

(continued)

		Case 6			Case 7				Case 8				Case 9				Case 10			
		SC	NL	AS	SC	NL	AS	PrP	SC	NL	AS	PrP	SC	NL	AS	PrP	SC	NL	AS	PrP
Mesencephalon	Superior colliculus	+	+	+	+	+	+	+	+	+	+	+	+	+	+	+		+	+	++
	Inferior colliculus	+	+	+	+	+	+	−	NE	NE	NE	NE	NE	NE	NE	NE	−	+	+	++
	Periaqued. gray matter	−	±	+	+	−	+	+	+	−	+	±	+	±	+	+	−	−	+	+
	Oculomotor nucleus	−	−	−	−	−	−	−	±	−	±	±	+	−	+	±	+	−	−	+
	Red nucleus	−	−	+	−	−	−	−	±	−	±	±	+	−	+	−	−	−	−	−
	Reticular formation	−	−	+	+	−	+	−	±	−	±	±	+	−	+	±	±	−	±	+
	Subst. nigra. Z. comp.	−	+	−	−	+	±	−	±	+	+	±	−	−	±	+	+	±	±	+
	Subst. nigra. Z. reticu.	−	+	+	−	+	±	−	−	−	+	−	−	−	±	±	+	±	±	+
Pons	Locus ceruleus	−	−	−	−	−	−	−	±	−	±	+	−	−	±	+	−	−	−	+
	Raphe nucleus	−	−	−	−	−	−	+	−	−	−	+	+	±	+	±	−	−	−	+
	Reticular formation	−	−	−	−	−	−	+	±	−	±	+	+	−	+	±	−	−	−	+
	Pontine nuclei	−	+	+	−	+	+	±	±	+	+	+	±	±	+	+	+	++	++	+
Medulla oblongata	Nucl. N. hypogloss.												±		±					+
	Nucl. dors. n. trigem.	−	−	−	−	−	−	−	−	−	−	±	−	−	−	−	−	−	−	+
	Nucl. tr. spin. n. trigem.	−	−	−	−	−	−	−	−	−	−	±	+	−	+	−	−	−	−	+
	Raphe nucleus	−	−	−	−	−	−	−	−	−	−	±	±	−	±	−	−	−	−	+
	Reticular formation	−	−	−	−	−	−	−	−	−	±	±	+	−	+	+	−	−	+	+
	Olivary nucleus	−	+	+	−	+	+	+	−	+	+	+	+	+	+	+	−	−	+	++
	Nucl. fasc. poster.										+		+		+					++

AS, astrocytosis; NE, not examined; NL, neuronal loss; PrP, prion protein; SC, spongiform change.

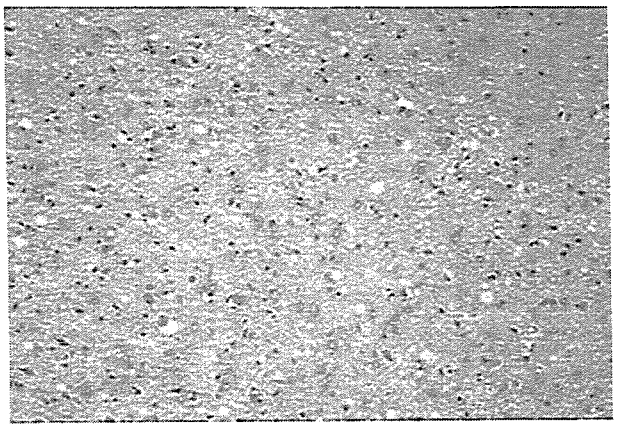

Fig. 1 Spongiform changes of moderate degree associated with neuronal loss and proliferation of hypertrophic astrocytes in the superior colliculus (case 8, HE stain).

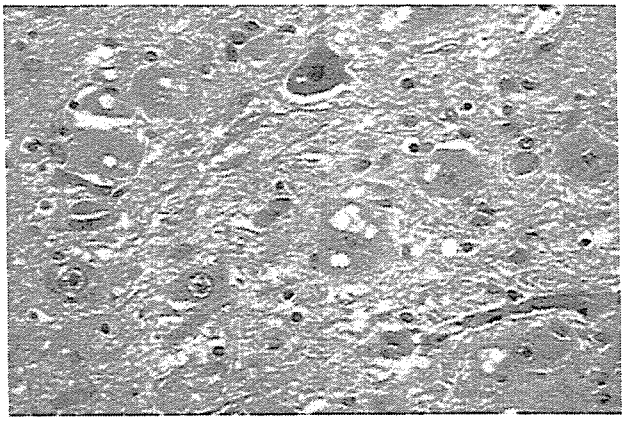

Fig. 2 Multiple large vacuoles found in the neuronal perikarya in the oculomotor nucleus (case 9, HE stain).

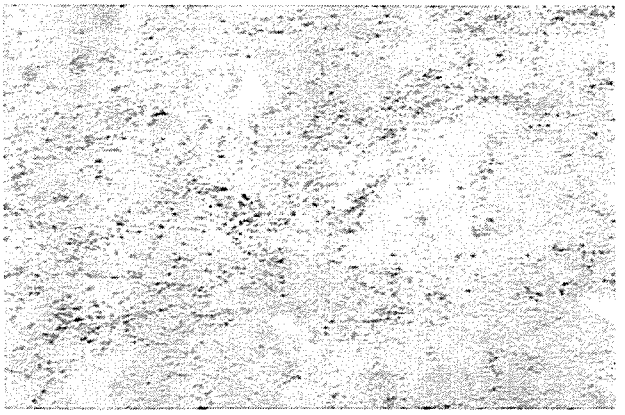

Fig. 3 Diffuse or synaptic type immunoreactivity against PrP in the neuropil of the superior colliculus (case 1, immunostain for PrP).

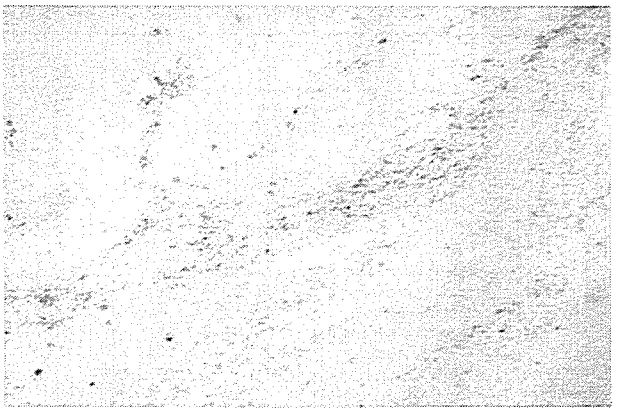

Fig. 5 Prominent deposition of PrP of diffuse or synaptic type in the pontine nuclei (case 8, immunostain for PrP).

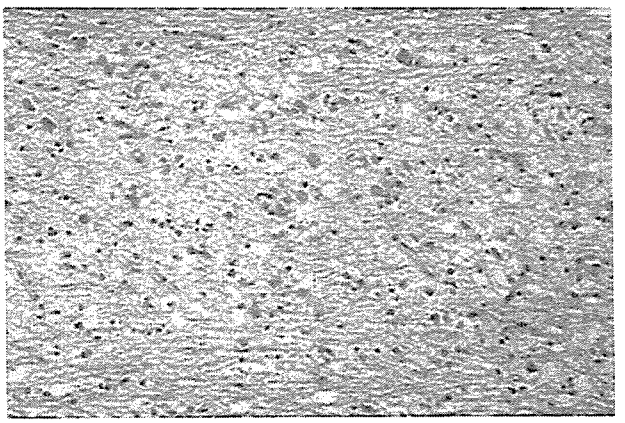

Fig. 4 Severe neuronal loss associated with spongiform changes and astrocytosis in the pontine nuclei. The sizes of the perikarya of the remaining neurons are reduced (case 10, HE stain).

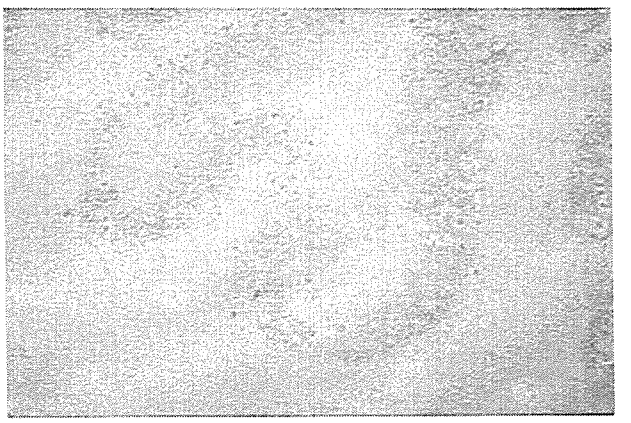

Fig. 6 Neurons of the inferior olivary nucleus were well preserved, but marked deposition of PrP was found in the neuropil (case 10, immunostain for PrP).

occasionally found in the zona reticulata, showing mild astrocytosis.

Diffuse or synaptic-type immunoreactivity against PrP was consistently found in the quadrigeminal plate (Fig. 3), while it was weak or absent in other regions of the mesencephalon, and it roughly paralleled neuronal loss and astrocytosis.

Pons

The histopathological alterations in the pons were almost restricted to the pontine base except for case 9, and the tegmentum was well preserved as a whole. In case 9, spongiform changes accompanied by astrocytosis were seen in the reticular formation and raphe nucleus without apparent neuronal loss. The pontine base was affected in nine of the ten cases, and the loss of neurons of moderate to marked degree in association with hypertrophic astrocytosis was observed in the pontine nuclei (Fig. 4), while spongiform changes in the pontine nuclei were observed only in cases 5 and 10. The sizes of the perikarya of the remaining neurons in the pontine nuclei were reduced as a whole.

Diffuse or synaptic-type immunoreactivity against PrP was noted throughout all gray matter structures in the pons except in case 4, but was most prominent in the pontine nuclei (Fig. 5).

Medulla oblongata

The medulla oblongata was essentially histopathologically normal in all cases. In case 9, only mild spongiform changes accompanied by astrocytosis were noted throughout all

gray matter structures of the medulla oblongata, but no neuronal loss was observed in the tegmentum. The inferior olivary nucleus showed mild neuronal loss and astrocytosis in six cases, but these changes were considered most likely to be an age-related phenomenon and not of pathological nature. Axonal spheroids (dystrophic axon terminals) were consistently found in the gracile nucleus.

The results of anti-PrP immunohistochemistry, which was performed in four cases, were not anticipated based on the histopathological findings. Distinct, diffuse or synaptic-type immunoreactivity was noted throughout the inferior olivary nucleus in every case (Fig. 6). In addition, the tegmental structures showed diffuse immunoreactivity in case 10.

DISCUSSION

In sporadic CJD, the brain stem is comparatively spared from pathological alterations, and this is a characteristic of sporadic CJD,[1,4,5] a condition which is distinct from kuru[6,7] or prion diseases in animals such as scrapie[8] and BSE[9] in which the brain stem is severely affected. A previous western immunoblot analysis of the intracerebral distribution of infectious amyloid protein (PrP) in human spongiform encephalopathy revealed the almost complete absence of amyloid protein in the brain stem in sporadic CJD.[14] On the other hand, in variant CJD spongiform changes are occasionally found in the periaqueductal gray matter and pontine nuclei, and neuronal loss with astrocytosis can be seen in structures such as the superior and inferior colliculi, periaqueductal gray matter, inferior olivary nucleus and dorsal vagal nucleus.[12] It is unknown at present why this difference in the distribution of lesions occurs among various kinds of prion disease. In sporadic CJD, the brain stem is less vulnerable or resistant to lesions caused by PrP. It is therefore intriguing to observe in full detail the pathological alterations of the brain stem in sporadic CJD, because progression of the disease might be slower in the brain stem than in the cerebral or cerebellar cortex. By close observation of the brain stem lesions, we might be able to determine the pathological changes in the early stages of the disease.

The results obtained in the present study supported the general view that the brain stem lesions are of mild degree in sporadic CJD. However, on closer examination, some specific and non-specific lesions of variable degree were found at various sites, and this is a phenomenon which is similar with the lesions seen in the hippocampus in sporadic CJD.[15] We discuss some of the brain stem lesions observed and make brief comments on each topic below.

1 We adopted three histopathological parameters[1,2] to evaluate the brain stem lesions, spongiform changes of the neuropil, neuronal loss and hypertrophic astrocytosis, but they did not necessarily occur in parallel. While the proliferation of astrocytes was noted in almost all lesions, it did not accompany neuronal loss in some regions, and spongiform changes were not apparent in the brain stem in most cases except for in the quadrigeminal plate and substantia nigra. Whereas spongiform changes in CJD are generally regarded an early event which precedes neuronal loss and astrocytosis,[4] astrocytosis was observed to occur before the appearance of spongiform changes in experimentally transmitted scrapie.[16] The proliferation of hypertrophic astrocytes therefore might not simply be a secondary change. (It should be also noted that the intensity of immunoreactivity against PrP did not parallel the histopathological alterations. In many regions, for example the pontine tegmentum and inferior olivary nucleus, the deposition of PrP was noted without accompanying spongiform changes or neuronal loss. This might indicate that these brain stem structures are resistant to the pathological processes induced by PrP.)

2 In the mesencephalon, the superior and inferior colliculi are consistently vulnerable in sporadic CJD, and similar involvement of the quadrigeminal plate was previously noted by some authors.[4] While the substantia nigra was affected in most cases, the changes were relatively mild. A few senile plaques were found in the periaqueductal gray matter in one case (case 1). Although the occurrence of amyloid plaques with a wide morphological spectrum has been previously documented in the mesencephalon of some cases of sporadic CJD,[5] the plaques in our case were immunohistochemically negative for PrP and probably represented a senile change.

3 The formation of large vacuoles in the perikarya of neurons has previously been consistently observed in the brain stem, especially in the medulla oblongata, in BSE[9,17] and scrapie,[8] and is pathognomonic for these disorders. Perikaryal vacuole formation is not a prominent feature in the cerebral or cerebellar cortex in sporadic CJD. On the other hand, it is commonly observed in the brain stem in kuru.[6,7] In the present study, this was seen in the oculomotor nucleus in two cases and in the substantia nigra in another case, without being accompanied by neuronal loss.

4 In the pontine base, although spongiform changes of the neuropil were found in only two cases, neuronal loss with astrocytosis of moderate to marked degree was noted in the pontine nuclei in most. The deposition of PrP was also observed in five of eight cases. It is certain that the pontine nuclei are sites which are consistently affected by the pathological processes that occur in sporadic CJD, and this is in accordance with the observations of Tateishi *et al.*[5] Recently Iwasaki *et al.*[10] also described gross atrophy of the pontine base, neuronal loss and prominent PrP immunoreactivity in the pontine nuclei in most cases of sporadic CJD, and similar results were also obtained for variant CJD.[12]

The sizes of the perikarya of the remaining neurons in the pontine nuclei appeared to be generally reduced in our series. Because the sizes of the neuronal perikarya show considerable regional variation within the pontine nuclei,[18] a more strict quantitative study is needed to confirm this observation. Neurons of the pontine nuclei send their axons to the cerebellar granule cell layer and also receive many fibers from the broad regions of the cerebral cortex.[18] Therefore, the possibility is considered that the atrophy of the neuronal perikarya in the pontine nuclei was partly caused by anterograde and/or retrograde trans-synaptic degeneration, as suggested by Tateishi *et al.*[5]

5 The medulla oblongata was preserved in an approximately normal state histopathologically except for one case. In thalamic type of CJD, severe degeneration of the inferior olivary nucleus constantly occurs.[19,20] In the present series, no case of thalamic type CJD was included and degeneration of the inferior olivary nucleus was not noted. However, in spite of the absence of pathological neuronal loss, the deposition of PrP was consistently found in the inferior olivary nucleus.

In recent years, the variability of clinicopathological phenotypes in patients with sporadic CJD has been demonstrated to depend on a polymorphism at codon 129 of the *PrP* gene as well as a pattern on Western immunoblot analysis of PrP, and a new classification scheme based upon these data is widely being employed.[21] Because the present study is a retrospective one that was performed on archival autopsy materials, the results of molecular analysis of PrP and its gene were not available for most of the cases. This is a major limitation of our study, and an investigation for the correlation of the molecular characteristics of PrP and pathological findings of brain stem lesions in sporadic CJD should be performed in future studies. At this stage, very limited inference can be made on the genotypes of *PrP* in the present series. Judging from the fact that in more than 90% of the Japanese population codon 129 of the *PrP* gene is homozygous for methionine (MM type) and also judging from the clinicopathological features of each patient in our series (periodic synchronous discharge was observed on electroencephalogram in all patients), it is supposed that most of our cases 1–7 are probably the MM1 type.

The relationship between the histopathological and immunohistochemical findings of the brain stem and the duration of the clinical course is another problem that remains to be elucidated. In the present series, the severity of the histopathological findings and the regional distribution of the immunohistochemical reactivity of PrP varied from case to case, and we could not find a clear correlation between the duration of the clinical course and these findings in the brain stem lesions.

In summary, we showed that in sporadic CJD pathological alterations of variable degree were observed in the brain stem, in particular in the quadrigeminal plate and pontine nuclei, although spongiform changes were found only infrequently. The medulla oblongata did not show any significant histopathological lesions. The deposition of PrP was mainly observed in the quadrigeminal plate and pontine nuclei. We also noted this in the pontine tegmentum and inferior olivary nucleus, which appeared to be approximately normal by histopathological examination. The remaining problems include the relationships between these changes in the brain stem and the lesions in the cerebellum, the possibility of trans-synaptic degeneration of neurons in the pontine nuclei, the clinical significance of these brain stem lesions, and the reasons for the differences between the lesions of the brain stem in sporadic CJD and those in kuru or variant CJD.

REFERENCES

1. Budka H, Aguzzi A, Brown P *et al.* Neuropathological diagnostic criteria for Creutzfeldt-Jakob disease (CJD) and other human spongiform encephalopathies (prion diseases). *Brain Pathol* 1995; **5**: 459–466.
2. Ironside JW. Review. Creutzfeldt-Jakob disease. *Brain Pathol* 1996; **6**: 379–388.
3. Mizutani T, Okumura A, Oda M, Shiraki H. Panencephalopathic type of Creutzfeldt-Jakob disease. Primary involvement of the cerebral white matter. *J Neurol Neurosurg Psychiat* 1981; **44**: 103–115.
4. Masters CL, Richardson EP Jr. Subacute spongiform encephalopathy (Creutzfeldt-Jakob disease). The nature and progression of spongiform change. *Brain* 1978; **101**: 333–344.
5. Tateishi J, Sato Y, Ohta M. Creutzfeldt-Jakob disease in humans and laboratory animals. *Progr Neuropathol* 1983; **5**: 195–221.
6. Klatzo I, Gajdusek DC, Zigas V. Pathology of kuru. *Lab Invest* 1959; **8**: 799–847.
7. Hainfellner JA, Liberski PP, Guiroy DC *et al.* Pathology and immunocytochemistry of a kuru brain. *Brain Pathol* 1997; **7**: 547–553.
8. Wood JLN, McGill IS, Done SH, Bradley DR. Neuropathology of scrapie. A study of the distribution patterns of brain lesions in 222 cases of natural scrapie in sheep, 1982–1991. *Vet Rec* 1997; **140**: 167–174.
9. Wells GAH, Wilesmith JW. The neuropathology and epidemiology of bovine spongiform encephalopathy. *Brain Pathol* 1995; **5**: 91–103.
10. Iwasaki Y, Sobue G, Yoshida M, Hashizume Y. Neuropathological characteristics of brainstem lesions in sporadic Creutzfeldt-Jakob disease. *Brain Pathol* 2003; **13**: s149.

11. Will RG, Ironside JW, Zeidler M *et al.* A new variant of Creutzfeldt-Jakob disease in the UK. *Lancet* 1996; **347**: 921–925.
12. Ironside JW, Head MW, Bell JE, McCardle L, Will RG. Laboratory diagnosis of variant Creutzfeldt-Jakob disease. *Histopathol* 2000; **37**: 1–9.
13. Kitamoto T, Shin RW, Doh-ura K *et al.* Abnormal isoform of prion proteins accumulates in the synaptic structures of the central nervous system in patients with Creutzfeldt-Jakob disease. *Am J Pathol* 1992; **140**: 1285–1294.
14. Brown P, Kenney K, Little B *et al.* Intracerebral distribution of infectious amyloid protein in spongiform encephalopathy. *Ann Neurol* 1995; **38**: 245–253.
15. Mizusawa H, Hirano A, Llena JF. Involvement of hippocampus in Creutzfeldt-Jakob disease. *J Neurol Sci* 1987; **82**: 13–26.
16. Wiley CA, Burrrola PG, Buchmeier MJ *et al.* Immunogold localization of prion filaments in scrapie-infected hamster brains. *Lab Invest* 1987; **57**: 646–656.
17. Wells GAH, Hancock RD, Cooley WA, Richards MS, Higgins RJ, David GP. Bovine spongiform encephalopathy. Diagnostic significance of vacuolar changes in selected nuclei of the medulla oblongata. *Vet Rec* 1989; **125**: 521–524.
18. Carpenter MB, Sutin J. *Human Neuroanatomy*, 8th edn. Baltimore/London: Williams & Wilkins, 1983.
19. Mizusawa H, Ohkoshi N, Sasaki H, Kanazawa I, Nakanishi T. Degeneration of the thalamus and inferior olives associated with spongiform encephalopathy of the cerebral cortex. *Clin Neuropathol* 1988; **7**: 81–86.
20. Kornfeld M, Seelinger DF. Pure thalamic dementia with a single focus of spongiform change in cerebral cortex. *Clin Neuropathol* 1994; **13**: 77–81.
21. Parchi P, Castellani R, Capellari S *et al.* Molecular basis of phenotypic variability in sporadic Creutzfeldt-Jakob disease. *Ann Neurol* 1996; **39**: 767–778.

Surface Plasmon Resonance Analysis for the Screening of Anti-prion Compounds

Satoshi KAWATAKE,[a] Yuki NISHIMURA,[a] Suehiro SAKAGUCHI,[b] Toru IWAKI,[c] and Katsumi DOH-URA*,[a]

[a] *Department of Prion Research, Tohoku University; Sendai 980–8575, Japan:* [b] *Department of Molecular Microbiology and Immunology, Nagasaki University; Nagasaki 852–8523, Japan: and* [c] *Department of Neuropathology, Neurological Institute, Kyushu University; Fukuoka 812–8582, Japan.*

Received November 2, 2005; accepted January 24, 2006; published online January 27, 2006

The interaction of anti-prion compounds and amyloid binding dyes with a carboxy-terminal domain of prion protein (PrP121—231) was examined using surface plasmon resonance (SPR) and compared with inhibition activities of abnormal PrP formation in scrapie-infected cells. Most examined compounds had affinities for PrP121—231: antimalarials had low affinities, whereas Congo red, phthalocyanine and thioflavin S had high affinities. The SPR binding response correlated with the inhibition activity of abnormal PrP formation. Several drugs were screened using SPR to verify the findings: propranolol was identified as a new anti-prion compound. This fact indicates that drug screenings by this assay are useful.

Key words anti-prion compound; surface plasmon resonance; scrapie-infected cell; screening; recombinant prion protein

Transmissible spongiform encephalopathies or prion diseases are fatal neurodegenerative disorders that include Creutzfeldt–Jakob disease and Gerstmann–Sträussler–Scheincker syndrome in humans, and scrapie, bovine spongiform encephalopathy and chronic wasting disease in animals. These disorders are characterized by accumulation in the brain of an abnormal isoform of prion protein (PrP), which includes a high beta-sheet content and is resistant to digestion with proteinase K.[1] Recent outbreaks of variant Creutzfeldt–Jakob disease[2] and iatrogenic Creutzfeldt–Jakob disease through use of cadaveric growth hormone or dura grafts[3] in younger people have necessitated the development of suitable therapies. Compounds such as antimalarials and amyloid binding dyes are known to possess anti-prion activity *in vitro* or *in vivo*.[4—14] Among them, Congo red and quinacrine are known to bind directly to PrP and thereby strongly inhibit proteinase K-resistant PrP (PrPres) formation.[15,16] However, it remains unclear whether or not other anti-prion compounds and amyloid binding dyes interact directly with PrP. This study analyzed interactions of some previously reported anti-prion compounds[4,7,11,17,18] and popularly used amyloid binding dyes with recombinant PrP using surface plasmon resonance (SPR). In addition, we evaluated whether SPR assay is useful as a screening tool for anti-prion compounds.

MATERIALS AND METHODS

Compounds Compounds used in the study (Fig. 1) were obtained from Sigma Aldrich Corp. (quinacrine dihydrochloride (QC, MW: 400.0), quinine hydrochloride (QN, MW: 324.4), thioflavin T (ThT, MW: 283.4, dye content 65%), thioflavin S (ThS, MW: undetermined), propranolol (MW: 295.8), promethazine hydrochloride (MW: 284.4), carbamazepine (MW: 236.3) and theophylline (MW: 180.2)), Aldrich (chloroquine diphosphate (CQ, MW: 319.9), and Congo red (CR, MW: 696.7, dye content 97%)), ICN (phthalocyanine tetrasulfonate (PcTS, MW: 922.7)), Wako Pure Chemical Industries Ltd. (Tokyo, Japan) (tetracycline hydrochloride (TC, MW: 444.4), diazepam (MW: 284.7), folic acid (MW: 441.4) and phenytoin (MW: 252.3)) or Nacalai Tesque (Tokyo, Japan) (testosterone (MW: 288.4)). All compounds were prepared as 20 mM stock solutions in water or dimethyl sulfoxide.

SPR Analysis The SPR analysis was performed using an

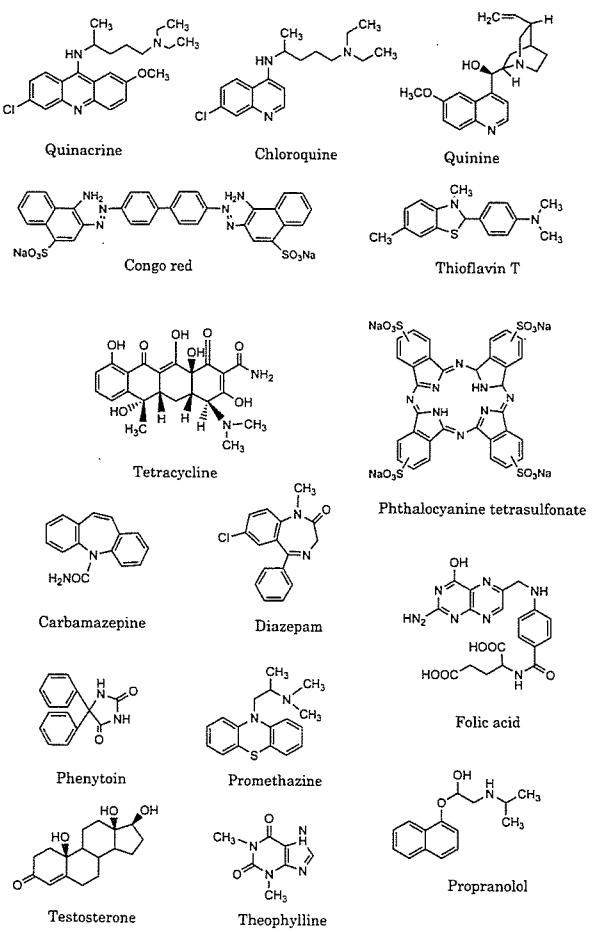

Fig. 1. Structures of Compounds or Drugs Used in the Study

* To whom correspondence should be addressed. e-mail: doh-ura@mail.tains.tohoku.ac.jp

optical biosensor (Biacore AB, Uppsala, Sweden) equipped with a CM5 sensor chip. Recombinant mouse PrP was prepared as described previously[19,20] and immobilized on a biosensor chip at a density of *ca.* 3000 resonance units (RU) using amine coupling.[21] Test compounds were diluted to 100 μM with running buffer (70 mM NaCl, 53 mM Na_2HPO_4, 12.5 mM KH_2PO_4, pH 7.4) and contained 0.5% DMSO. After they were confirmed to be in solution without precipitation or aggregation, they were injected over the PrP flow cell and the reference for either 60 s at a flow rate of 20 μl/min (low-affinity compounds) or 90 s at a flow rate of 30 μl/min (high-affinity compounds). The dissociation phase was monitored for 60 s (low-affinity compounds) or 270 s (high-affinity compounds). The flow cell was washed with 10 mM NaOH or 0.01% Triton X-100 for 30 s between each sample injection. Buffer blanks for double referencing were injected before sample analyses.[22]

The full-length recombinant of mouse PrP (residues 23—231) was used initially in the experiment, but it was easily degraded during SPR analysis in the amino-terminal portions attributable to an unidentified mechanism. For that reason, the carboxy-terminal polypeptide (residues 121—231; PrP121—231), which represents the only autonomous folding unit of PrP with a defined three-dimensional structure,[19,23,24] was used in this study.

Every PrP-immobilized biosensor chip used in the study was confirmed to respond almost the same and was standardized by the measurement of QC before its use for sample analyses.

Data Analysis The binding response, which is an index for estimating the interaction of a compound with molecules sited on a biosensor chip, is obtained from the equilibrium response (R_{eq}) value or the maximum response value in the sensorgram divided by the molecular weight.[25] In this study, the binding response of a compound was standardized by calibrating with QC, whose binding response was designated as 100 RU/Da. For low-affinity compounds, the dissociation constant (K_D) based on the R_{eq} state was calculated from data at doses ranging from 10 μM to 1 mM by either steady-state analysis using BIAevaluation software (ver. 3.0; Biacore AB) or Scatchard plot analysis. On the other hand, the K_D for high-affinity compound CR or PcTS was deduced after the data were fit to a binding model assuming a bivalent analyte in BIAevaluation software. The fitting was performed in such a way that the χ^2 value representing the statistical closeness of curve-fitting became the lowest. It was recommended ideally to be below 10.

Statistical linear correlation was evaluated using Pearson's correlation coefficient; Fisher's r to z method was used to calculate the p values. Simple linear regression analysis was also performed.

Anti-prion Activity Assay Anti-prion activity of a compound was assayed by measuring its 50% inhibition doses (IC_{50}) for PrPres formation in scrapie-infected neuroblastoma (ScNB) cells as described in previous reports.[7,11,12] Briefly, compounds were added at designated concentrations to the medium when cells were passed at 10% confluency. Cells were allowed to grow to confluence and lysed with lysis buffer (0.5% sodium deoxycholate, 0.5% Nonidet P-40, PBS). Lysates were digested with 10 μg/ml proteinase K for 30 min and centrifuged at 100000×g for 30 min at 4 °C. The pellets were resuspended in sample loading buffer and boiled. Samples were separated using electrophoresis on a 15% Tris-glycine-SDS-polyacrylamide gel and electroblotted. PrPres was detected using an antibody SAF83 (1 : 5000; SPI-Bio, France), followed by an alkaline phosphatase-conjugated secondary antibody. Immunoreactive signals were visualized using CDP-Star detection reagent (Amersham Biosciences Corp., U.S.A.) and were analyzed densitometrically. Three independent assays were performed in each experiment.

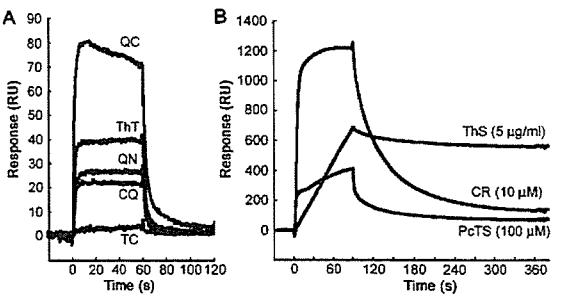

Fig. 2. Interactions of Anti-prion Compounds with PrP121—231

(A) Sensorgrams of the low-affinity compounds quinacrine (QC), chloroquine (CQ), quinine (QN), thioflavin T (ThT) and tetracycline (TC), all at 100 μM. (B) Sensorgrams of the high-affinity compounds Congo red (CR, 10 μM), phthalocyanine tetrasulfonate (PcTS, 100 μM) and thioflavin S (ThS, 5 μg/ml).

RESULTS

Interaction of Anti-prion Compounds with PrP The SPR sensorgrams of ThT and antimalarials such as QC, QN and CQ (each at 100 μM) demonstrated weak signal responses of less than 100 RU (Fig. 2A). The responses of these compounds reached equilibrium (R_{eq}) within a few seconds and returned to the baseline very rapidly after dissociation. These sensorgrams were typical for low-affinity interactions: TC showed almost no response. On the other hand, all sensorgrams of high-affinity compounds, such as CR, PcTS and ThS, showed much stronger responses and individual characteristic curves that differed from those of the low-affinity compounds (Fig. 2B). The CR (10 μM) showed the strongest signal, which was greater than 1200 RU: this decreased very slowly in the dissociation phase. The signal responses for PcTS (100 μM) and ThS (5 μg/ml) showed that neither reached the R_{eq} state within the association phase or returned to the baseline within the dissociation phase. In particular, ThS was only slightly dissociated and remained bound. This sensorgram resembled the sensorgram of biquinoline, an effective inhibitor of PrPres formation in ScNB cells (IC_{50}=3 nM).[11]

K_D Determination The dose response curve for QC appeared to be monophasic and to reach a saturation level at higher concentrations; its dissociation constant (K_D) value was calculated as 1.1 mM or 0.9 mM using steady-state analysis or Scatchard plot analysis, respectively (Figs. 3A—C). Vogtherr *et al.*[16] reported the dissociation constant (K_D= 4.6 mM) of the complex of QC and human PrP 121—230 analyzed by nuclear magnetic resonance (NMR) spectroscopy. This value was almost comparable to the K_D value obtained in this study, indicating that the method used in this study was relevant. The other two low-affinity compounds, QN and

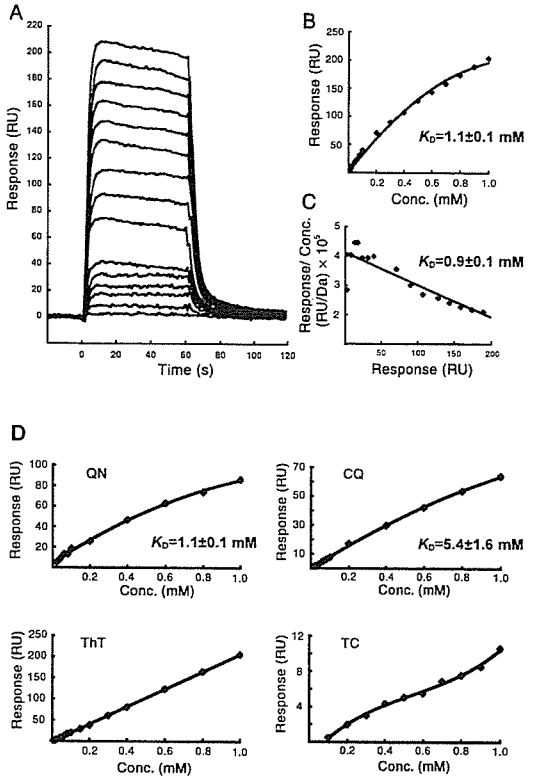

Fig. 3. Kinetic Analyses of Low Affinity Compounds

(A) Sensorgrams, (B) dose response curve and (C) scatchard plot of QC. (D) Dose response curves of QN, CQ, ThT, and TC.

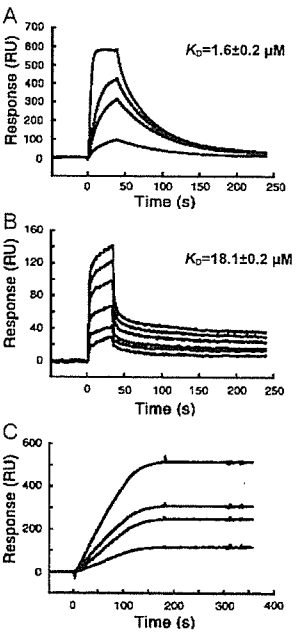

Fig. 4. Kinetic Analyses of High Affinity Compounds

(A) Sensorgrams of CR at concentrations of 1, 2, 3.3 and 5 μM, and its K_D value. (B) Sensorgrams of PcTS at concentrations of 1, 5, 10, 50, 75 and 100 μM, and its K_D value. (C) Sensorgrams of ThS at concentrations of 1, 2, 3 and 5 μg/ml, and its K_D value could not be calculated because of its undetermined structure and molecular weight.

CQ, respectively showed a similar monophasic pattern in dose response curves, yielding K_D of 1.1 mM and 5.4 mM (Fig. 3D). These K_D values, however, were of rough estimation and might be a little underscored due to lack of the data at concentrations of more than 1 mM. Unstable solubility of the compounds at such high concentrations hindered further analyses.

On the other hand, ThT gave a linear dose–response curve within a concentration of up to 1 mM and TC showed a biphasic pattern (Fig. 3D). Therefore, the saturation levels and K_D values of these compounds could not be determined, indicating that these compounds have a very low or no affinity with PrP121—231. Of them, TC is known to revert abnormal physicochemical properties of PrPres *in vitro*,[18] and interaction between TC and human PrP 106—126 peptides is revealed by NMR analysis.[26] Their data appear to be inconsistent with the data in this study. However, this discrepancy might be attributable to the lack of a TC binding site in the PrP121—231 used in our study.

Each sensorgram of high affinity compounds showed a very slow dissociation phase and was individually characteristic (Fig. 4). The structural and stoichiometric binding details of the compounds with PrP121—231 have not yet been established, but CR or PcTS is a symmetrical molecule and either half of the molecule has anti-prion activity (Doh-ura K, unpublished data). Consequently, the K_D value for the compound was deduced after the data were fit to a binding model assuming a bivalent analyte. The K_D of CR was calculated to be 1.6 μM from the sensorgrams of 1, 2, 3.3 and 5 μM (χ^2=20.9±2.1) (Fig. 4A). The K_D of PcTS was calculated as 18.1 μM from the sensorgrams of 1, 5, 10, 50, 75 and 100 μM (χ^2=28.1±2.9) (Fig. 4B). The K_D of ThS was incalculable to an exact degree because it is presumed to be a mixture of compounds formed by methylation and sulfonation of primulin; their structures and molecular weights have not been determined.

Comparison between PrP Affinity and Anti-prion Activity The IC_{50} value for the inhibition of PrPres formation in ScNB cells, either previously reported or examined in this study, was used as an anti-prion activity in this study. It was compared with the K_D or with the binding response. The latter, an index for estimating the interaction, was obtained from the R_{eq} value or the maximum response value at a concentration of 1 mM divided by the molecular weight (Table 1).

From data of all compounds except ThT, TC and ThS, statistical analyses demonstrated a significant linear correlation between the reciprocal of binding response and the IC_{50} (r=0.985, p=0.0005) (Fig. 5). This relation appeared to be also observed in TC, but not in ThT showing the next highest binding response to QC but no inhibition of PrPres formation within a non-toxic dose range. However, ThT demonstrated cell-toxicity at such a low dose as 0.05 μM.

For ThS, assuming that its minimum molecular weight deduced from presumable structures was 520 Da, its binding response was estimated to be 5.03 RU/Da; the IC_{50} was estimated to be about 2 μM, corresponding to about 1 μg/ml. However, these values seem to be underestimates because some constituents of ThS might interact with PrP121—231 or have inhibitory activity for PrPres formation. Therefore, active constituents of ThS might be expected to inhibit PrPres formation in ScNB cells at a submicromolar dose, similar to the other high-affinity compounds.

Screening by SPR Findings suggested that a compound

Table 1. Binding Response, Dissociation Constant (K_D) and 50% PrPres Inhibition Dose in ScNB Cells (IC_{50})

Compound	Binding response[a] (RU/Da)	K_D[b] (mM)	IC_{50}[c] (μM)
Low-affinity			
Quinacrine (QC)	0.25±0.00	1.1±0.1 (0.9±0.1)	0.3 (7)
Quinine (QN)	0.05±0.00	1.1±0.1 (1.4±0.1)	6.0 (11)
Chloroquine (CQ)	0.07±0.01	5.4±1.6 (3.5±0.8)	4.0 (7)
Thioflavin T (ThT)	0.16±0.01	n.d.[d] (n.d.[d])	No effect[f]
Tetracycline (TC)	0.01±0.00	n.d.[d] (n.d.[d])	No effect[g]
High-affinity			
Congo red (CR)	8.74±0.64	$1.6\pm0.2\times10^{-3}$	1.5×10^{-2} (4)
Phthalocyanine tetrasulfonate (PcTS)	1.82±0.06	$18.1\pm0.2\times10^{-3}$	0.5 (17)
Thioflavin S (ThS)	n.d.[e]	n.d.[e]	*ca.* 1 μg/ml

a) Binding response value was calculated from the R_{eq} value divided by the molecular weight for QC, QN, CQ and CR, or from the response value at a concentration of 1 mM divided by the molecular weight for ThT, TC and PcTS. *b*) K_D values were determined by steady state analysis for the low-affinity compounds or by bivalent analyte model analysis for CR and PcTS. K_D values from Scatchard plot analyses are shown in parentheses. *c*) IC_{50} values reported in the literature (reference shown in parentheses) or examined in this study. *d*) n.d.: not determined because a saturation level could not be estimated. *e*) n.d.: not determined because its structure and molecular weight were undetermined. *f*) Inhibition of PrPres formation was not observed up to a minimal toxic dose of 0.05 μM. *g*) Inhibition of PrPres formation was not observed up to a minimal toxic dose of 5.0 μM.

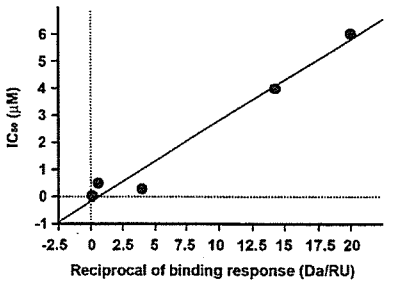

Fig. 5. Correlation between the Reciprocal of Binding Response and the IC_{50}

The data were from five compounds in which both binding response and IC_{50} were determined. Correlation showed a slope of 0.298, an intercept of −0.156 and a correlation coefficient of 0.971 (p=0.002) by simple linear regression analysis.

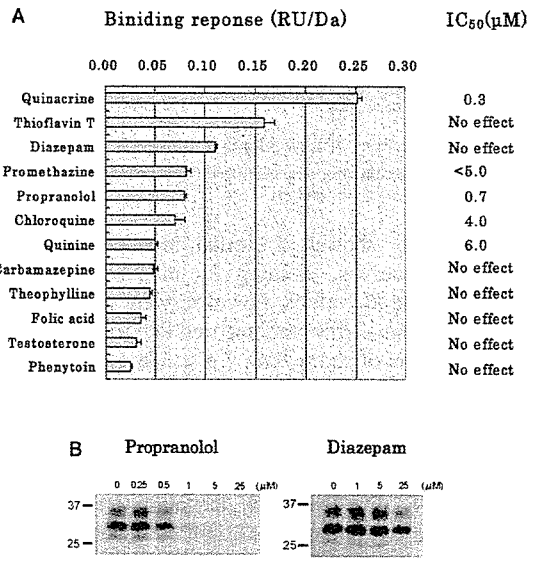

Fig. 6. Screening of Anti-prion Candidates Using the SPR Assay

(A) Binding response of each sample at 100 μM, and its IC_{50} of PrPres formation inhibition in ScNB cells within a non-toxic dose range. (B) Inhibition analyses of PrPres formation in ScNB cells grown in the presence with propranolol or diazepam. Molecular sizes in kDa are shown at the left of each panel.

capable of interacting with PrP121—231 might have a potency of inhibiting PrPres formation in ScNB cells. To verify this inference, several drugs were examined for either their binding response using the SPR method or their IC_{50} in ScNB cells. Eight clinically utilized drugs—carbamazepine, diazepam, folic acid, phenytoin, promethazine, propranolol, testosterone, and theophylline—all of which are low molecular weight compounds capable of crossing the blood brain barrier and share a partial structure similarity with the anti-prion compounds already reported, were examined and compared with the four anti-prion compounds (QC, QN, CQ, and ThT) (Fig. 6A).

Diazepam, promethazine and propranolol showed a higher binding response value than QN, which was the lowest binding response compound among the effective anti-prion compounds examined in this study. Among these, promethazine or propranolol inhibited PrPres formation in ScNB cells (propranolol: IC_{50}=0.7 μM; promethazine: IC_{50}<5.0 μM). Promethazine has already been reported to have anti-prion activity in ScNB cells,[8] whereas propranolol is a novel compound that inhibits PrPres formation in ScNB cells. Diazepam apparently did not inhibit PrPres formation within a non-toxic dose range up to 25 μM (Fig. 6B). Inhibitory activities against PrPres formation in ScNB cells were not observed for other drugs that had lower binding response values than QN.

DISCUSSION

We demonstrated that most anti-prion compounds examined in this study interacted with PrP121—231. The binding response of the compounds correlated with the IC_{50} of PrPres formation inhibition in ScNB cells. In addition, based on this finding, we proved that this interaction analysis using the SPR method was useful for screening to identify new candidates of anti-prion compounds. Three different *in vitro*